About the relation between the quasiparticle Green's function in cuprates obtained from ARPES data and the magnetic susceptibility

D.S. Inosov [a],[*], S.V. Borisenko [a], I. Eremin [b], A.A. Kordyuk [a],[c], V.B. Zabolotnyy [a],
J. Geck [a], A. Koitzsch [a], J. Fink [a], M. Knupfer [a], B. Büchner [a]

[a] *Institute for Solid State Research, IFW Dresden, P.O. Box 270116, D-01171 Dresden, Germany*
[b] *Max Planck Institute for the Physics of Complex Systems, D-01187 Dresden, Germany*
[c] *Institute of Metal Physics of National Academy of Sciences of Ukraine, 03142 Kyiv, Ukraine*

Available online 3 April 2007

Abstract

Angle resolved photoemission spectroscopy (ARPES) provides a detailed view of the renormalized band structure in cuprates and, consequently, is a key to the self-energy and the quasiparticle Green's function. Such information gives a clue to the comparison of ARPES with scanning tunneling microscopy, inelastic neutron scattering (INS), and Raman scattering data. Here we touch on a potential possibility of such a comparison with the dynamical magnetic susceptibility measured in INS experiments. Calculations based on the experimentally measured quasiparticle self-energies in cuprates lead to the estimated magnetic susceptibility response with many-body effects taken into account.
© 2007 Elsevier B.V. All rights reserved.

The normal-state Lindhard response function (polarization operator) is related to the quasiparticle Green's function via a simple autocorrelation formula [1]:

$$\chi_0(\mathbf{Q}, \Omega) \propto -2i \int G(\mathbf{k}, \omega) G(\mathbf{k} + \mathbf{Q}, \omega + \Omega) d^2k \, d\omega. \qquad (1)$$

Apart from the bare band structure, Eq. (1) also holds for the renormalized Green's function.

Knowing the Lindhard response function χ_0, one can obtain within random phase approximation (RPA) the dynamic spin susceptibility χ [2], the imaginary part of which is directly proportional to the measured INS intensity [3]:

$$\chi(\mathbf{Q}, \Omega) = \chi_0(\mathbf{Q}, \Omega)/[1 + J_\mathbf{Q}\chi_0(\mathbf{Q}, \Omega)]. \qquad (2)$$

The coefficient $J_\mathbf{Q}$ in the denominator of (2) describes the effective four-point vertex (Hubbard interaction or super-

exchange), which can be refined to the required degree of accuracy, although for many applications its k-dependence is neglected [4]. In our calculations we assume $J_\mathbf{Q} = J_0[\cos Q_x a + \cos Q_y a]$.

Following these formulae, it is straightforward to conclude that knowing the real and imaginary parts of the Green's function leads us to a comparison of ARPES results with the INS data. Although, this idea was discussed earlier [1,4–6], the calculations based on real ARPES data were not yet performed. The imaginary part of the Green's function is directly related to the measured ARPES intensity (although it can be affected by several factors). The real part can be obtained if one knows the self-energy, which is also a routine self-consistent Kramers–Kronig procedure in the state of the art ARPES data processing [7,8]. Thus, it is possible to calculate the magnetic susceptibility response from the experimental ARPES spectra.

In the superconducting (SC) state, the anomalous Green's function additionally contributes to χ_0, which cannot be

---
[*] Corresponding author.
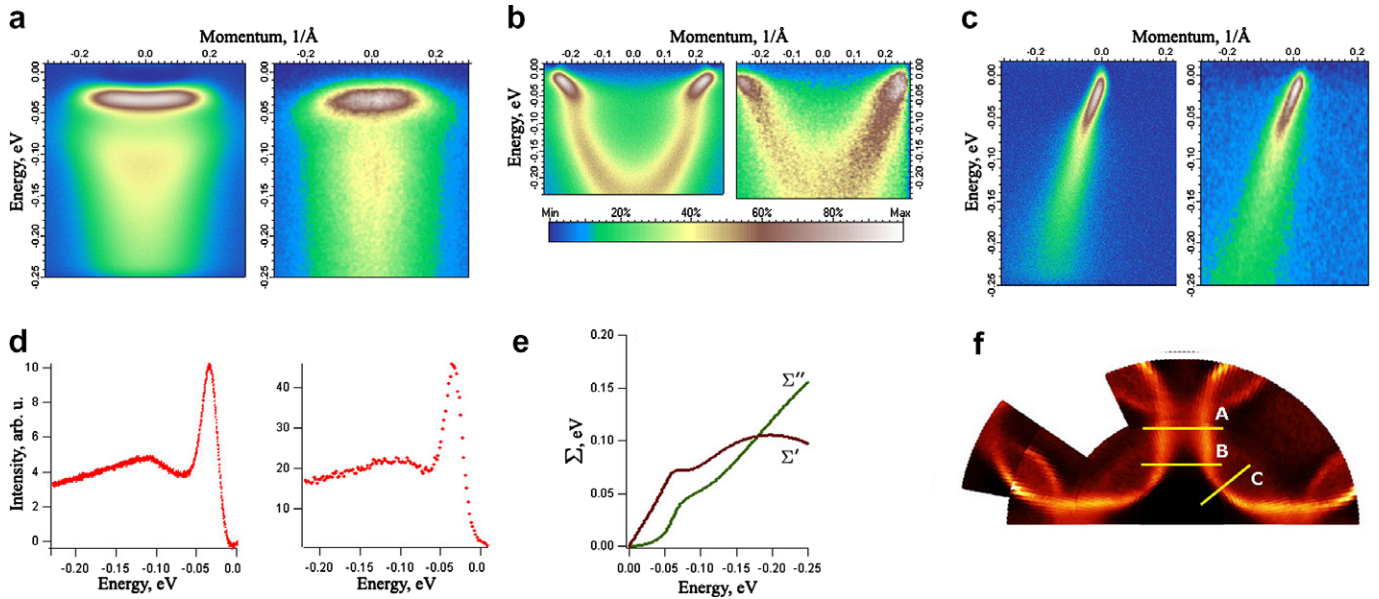*E-mail address:* d.inosov@ifw-dresden.de (D.S. Inosov).

Fig. 1. The modeled (left) and experimental (right) ARPES spectra of the antibonding band at $(\pi,0)$ point (a), along a shifted cut in the same direction (b) and along the (π,π) direction (c) in optimally doped Bi-2212 at 30 K. The model images correspond to the 20 meV energy resolution and 0.025 Å^{-1} angular resolution. (d) Modeled and experimental energy distribution curves at the $(\pi,0)$ point. (e) The Kramers–Kronig consistent real (Σ') and imaginary (Σ'') parts of the self-energy at (π,π) used in the calculation. (f) Positions of the cuts A–C in k-space.

taken into account from ARPES data. On the other hand, as this additional term is additive, we argue that all features observed in the first ("normal") term, including the resonance mode, will be still present in the resulting Lindhard function, so we content ourselves with the consideration of the first term only, even in the SC state.

In order to exclude the matrix elements effects and experimental resolution, we modeled the spectral function based on the bare electron dispersion studied in [8] and a self-energy model involving a quadratic scattering rate and coupling to a single k-dependent bosonic mode. The k-dependence of the density of states originating from the d-wave SC gap was also taken into account. The real part of the self-energy was calculated by the Kramers–Kronig procedure. Self-energy parameters were specified independently for the (π,π) and $(\pi,0)$ directions, with a d-wave interpolation between them. The SC gap was specified in the $(\pi,0)$ direction, vanishing in the d-wave manner towards (π,π). For posterior calculations, all the free parameters were adjusted during comparison with a set of experimental ARPES spectra in order to achieve the best correspondence (Fig. 1). For the details of the procedure see [9].

Basing on the model dataset built for optimally doped Bi-2212 at 50 K, with the SC gap of 30 meV, including bonding and antibonding bands with equal intensities, we have calculated the Lindhard function in the energy range down to 0.15 eV below the Fermi level in the whole Brillouin zone. After that we calculated the dynamical spin susceptibility by adjusting the J_0 parameter trying to reproduce the resonance at (π,π) and the 45° rotation of the incommensurate peaks that was most clearly observed
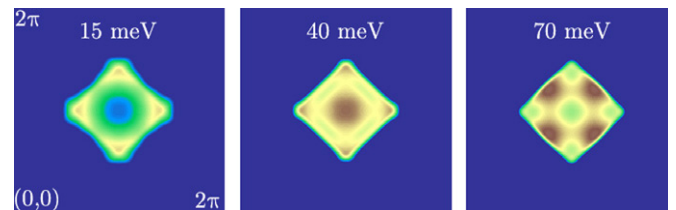

Fig. 2. Constant energy cuts of the dynamical spin susceptibility obtained from the renormalized Lindhard function within the RPA approach. The center of each Brillouin zone image corresponds to the (π,π) point.

in the INS experiments on YBCO [10]. The resulting χ (Fig. 2) qualitatively reproduces the energy resonance at ~40 meV in the (π,π) point, as well as the four peaks dispersing in the $(0,\pi)$ and $(\pi,0)$ directions below the resonance and along the Brillouin zone diagonals for higher energies.

Acknowledgement

References

[1] Ar. Abanov, A.V. Chubukov, Phys. Rev. Lett. 83 (1999) 1652.
[2] D.Z. Liu et al., Phys. Rev. Lett. 75 (1995) 4130.
[3] A. Schnyder et al., cond-mat/0510790 (2005).
[4] M.R. Norman, Phys. Rev. B 61 (2000) 14751.
[5] D. Manske et al., Phys. Rev. B 63 (2001) 054517.
[6] M. Norman, C. Pépin, Rep. Prog. Phys. 66 (2003) 1547.
[7] A.A. Kordyuk et al., Phys. Rev. B 67 (2003) 064504.
[8] A.A. Kordyuk et al., Phys. Rev. B 71 (2005) 214513.
[9] D.S. Inosov et al., cond-mat/0612040 (2006).
[10] S.M. Hayden et al., Nature 429 (2004) 531.